Atmos. Chem. Phys. Discuss., doi:10.5194/acp-2016-325, 2016
Manuscript under review for journal Atmos. Chem. Phys.
Published: 27 April 2016

Atmospheric Chemistry and Physics Discussions

What are the greenhouse gas observing system requirements for reducing fundamental biogeochemical process uncertainty? Amazon wetland CH_4 emissions as a case study.

A. Anthony Bloom[1], Thomas Lauvaux[1,2], Vineet Yadav[1], Riley Duren[1], Stanley Sander[1], John Worden[1], David Schimel[1].

[1]Jet Propulsion Laboratory, California Institute of Technology, Pasadena, CA

[2] Department of Meteorology, The Pennsylvania State University, University Park, PA

Correspondence to: A. Anthony Bloom (abloom@jpl.nasa.gov)

Abstract. Understanding the processes controlling terrestrial carbon fluxes is one of the grand challenges of climate science. Carbon cycle process controls are readily studied at local scales, but integrating local knowledge across extremely heterogeneous biota, landforms and climate space has proven to be extraordinarily challenging. Consequently, top-down or integral flux constraints at process-relevant scales are essential to reducing process uncertainty. Future satellite-based estimates of greenhouse gas fluxes – such as CO_2 and CH_4 – could potentially provide the constraints needed to resolve biogeochemical process controls at the required scales. Our analysis is focused on Amazon wetland CH_4 emissions, which amount to a scientifically crucial and methodologically challenging case study. We quantitatively derive the observing system requirements for testing wetland CH_4 emission hypotheses at a process-relevant scale. To capture the spatial and temporal patterns of the major hydrological and carbon controls over wetland CH_4 production, a satellite mission will need to resolve monthly CH_4 fluxes at a 300km resolution and with a 25% flux precision. We simulate a range of low-earth orbit (LEO) and geostationary orbit (GEO) CH_4 observing system configurations to evaluate the ability of these approaches to meet the CH_4 flux requirements. Conventional LEO and GEO missions resolve monthly 300km × 300km Amazon wetland fluxes at a 186% and 33% median uncertainty level. Improving LEO CH_4 measurement precision by $\sqrt{2}$ would only reduce the median CH_4 flux uncertainty to 132%. A GEO mission with targeted observing capability could resolve fluxes at a 21-27% median precision by increasing the observation density in high cloud-cover regions at the expense of other parts of the

Atmos. Chem. Phys. Discuss., doi:10.5194/acp-2016-325, 2016
Manuscript under review for journal Atmos. Chem. Phys.
Published: 27 April 2016

Atmospheric Chemistry and Physics Discussions

domain. Process-driven greenhouse gas observing system simulations can enhance conventional uncertainty reduction assessments by providing the measurement needs for testing biogeochemical process hypotheses.

1. Introduction

Quantitative knowledge of biogeochemical processes regulating global carbon-climate feedbacks remains highly uncertain (Friedlingstein et al., 2013). Quantifying the sensitivity of biogeochemistry to climate variables directly from observations of atmospheric concentrations has long been a goal of researchers (Bacastow et al., 1980; Vukicevic et al, 1997; Gurney et al., 2008). Estimating the climate sensitivity of carbon fluxes is complicated by both the spatial scale and structure of climate anomalies and the variations of factors affecting ecosystem responses: soils, vegetation, land use and natural disturbance (King et al., 2015). Current ground-based and even space-based carbon cycle observing systems produce flux estimates at continental or even zonal resolution, limiting direct estimation of relationships between climate forcing, ecosystem properties and carbon fluxes (Huntzinger et al., 2012, Peylin et al., 2013). The uncertainty of carbon fluxes at continental and finer scales is high, and different systems for flux estimation often produce strikingly different spatial patterns (Schimel et al 2015a; Bloom et al., 2016). Because of the high uncertainty in the spatial regionalization of fluxes, some of the most compelling studies of carbon and climate have eliminated the spatial information and instead have used correlative approaches to identify the regions likely to be responsible for observed global concentration anomalies (Braswell et al., 1997; Cox et al., 2013; Chen et al., 2015; Franklin et al., 2016).

The expansion of surface and aircraft observing networks has increased our understanding of the carbon cycle, and is essential for precise quantification of trace gas concentrations (Andrews et al., 2014, Sweeney et al., 2015; Wilson et al., 2016). Surface networks are intrinsically limited in their density, by cost, access to remote terrestrial and marine environments, environmental conditions and other logistical constraints (Schimel et al., 2015b). The first-generation trace gas observing satellites were designed to make global-scale measurements of concentrations with unprecedented frequency and accuracy, but were not designed to test specific hypotheses about biogeochemical processes. The successes of GOSAT (Yokota et al., 2009) and OCO-2 (Crisp et al., 2004) open the door to designing a next generation of spaceborne greenhouse

Atmos. Chem. Phys. Discuss., doi:10.5194/acp-2016-325, 2016
Manuscript under review for journal Atmos. Chem. Phys.
Published: 27 April 2016

Atmospheric Chemistry and Physics Discussions

gas measurements to test specific hypotheses about the terrestrial biosphere or the oceans. In this paper, we report an observing system design exercise aimed at identifying the observing system needed to increase understanding of a long-standing uncertainty in the global carbon budget, specifically the role of tropical wetlands in the global CH_4 budget (Mitsch et al., 2010; Bloom et al., 2010; Melton et al., 2013). While we focus this analysis on CH_4, we note that the models and methodology are equally applicable to other gases (such as CO_2), and other regions or mechanisms.

Wetland CH_4 emissions

Biogenic methane (CH_4) emission processes are one of the principal components of global carbon-climate interactions; CH_4 is a potent greenhouse gas (Myhre et al., 2013) and wetlands account for roughly 20-40% of the global CH_4 source (Kirschke et al., 2013). The processes controlling the magnitude and temporal evolution of CH_4 outgassing from wetland environments remain largely un-quantified on continental scales. As a result, global scale wetland CH_4 emissions (Melton et al., 2013) and their role in the inter-annual growth of atmospheric CH_4 remain highly uncertain.

Global wetland CH_4 emissions largely depend on soil inundation, temperature and substrate carbon availability. The major sources of wetland CH_4 emissions include boreal North America, boreal Eurasia, the Indonesian archipelago, the Congo and Amazon river basins (Figure 1, map) which are all characterized by high soil carbon content (Hiederer and Köchy, 2011) and substantial seasonal or year-round inundation extent (Prigent et al., 2012). By and large, Amazon wetland CH_4 emissions dominate both the magnitude and uncertainty of global wetland CH_4 emissions (Melton et al., 2013). Estimates of Amazon wetland CH_4 emissions range between 20 – 60 Tg CH_4 yr^{-1} (Fung et al., 1991; Riley et al., 2011; Bloom et al., 2012; Melack et al., 2004), roughly equivalent to 10 – 30% of the global wetland CH_4 source. Major uncertainties are also associated with the spatial and temporal variability of CH_4 emissions (Figure 1). Uncertainties in tropical wetland CH_4 emission estimates largely stem from a lack of quantitative knowledge of process controls on wetland CH_4 emissions, and a lack of data constraints on the drivers of wetland emissions. In terms of processes, a range of factors including soil pH, wetland vegetation cover, wetland depth, salinity and air-water gas exchange dynamics, likely impose fundamental controls on the

Atmos. Chem. Phys. Discuss., doi:10.5194/acp-2016-325, 2016
Manuscript under review for journal Atmos. Chem. Phys.
Published: 27 April 2016

rate of wetland CH_4 emissions. On a continental scale, spatially-explicit knowledge of carbon cycling and inundation remain highly uncertain in the wet tropics, primarily due to a sparse in-situ measurement network, high cloud cover and biomass density

Top-down CH_4 flux estimates

Top-down constraints on CH_4 fluxes – from atmospheric CH_4 observations – are key to retrieving quantitative information on continental-scale CH_4 biogeochemistry (Bousquet et al., 2011; Pison et al., 2013; Basso et al., 2016; Wilson et al., 2016). Low-earth orbit satellite missions, including SCIAMACHY, IASI, TES, and GOSAT have surveyed global CH_4 concentrations for over a decade (Frankenberg et al., 2008; Crevoisier et al., 2009; Butz et al., 2011; Worden et al., 2012). In particular, column CH_4 retrievals from SCIAMACHY have proven sensitive to wetland and other CH_4 emissions (Bloom et al., 2010; Bergamaschi et al., 2013). However, cloud cover is a major inhibiting factor when measuring atmospheric greenhouse gas concentrations within the proximity of tropical wetland regions. In particular, densely vegetated seasonally inundated areas of the Amazon and Congo river basins can experience more than 95% monthly mean cloud cover. With fewer cloud-free observations of lower tropospheric CH_4 concentrations, atmospheric inversion estimates of wetland CH_4 emissions remain exceedingly difficult, especially in the absence of well-characterized prior information on the magnitude, location and timing of emissions.

Atmospheric inverse estimates of CH_4 emissions are expected to improve with tropospheric CH_4 measurements from the upcoming ESA TROPOMI mission (Butz et al., 2012). Furthermore, geostationary missions (such as GEOCAPE) will potentially provide the measurements needed to substantially improve CH_4 emission estimates (Wecht et al., 2014; Bousserez et al., 2015). Ultimately, the precision and sampling configuration of atmospheric CH_4 observations both determine the observing system (OS) capability of retrieving surface CH_4 fluxes. It is currently unclear whether future CH_4 measurements will be sufficient to resolve key CH_4 fluxes – such as the Amazon basin wetlands – at a process-relevant resolution.

Atmos. Chem. Phys. Discuss., doi:10.5194/acp-2016-325, 2016
Manuscript under review for journal Atmos. Chem. Phys.
Published: 27 April 2016

Atmospheric Chemistry and Physics Discussions

In this study we characterize the satellite observations required to quantitatively resolve the processes controlling Amazon wetland CH_4 emissions. We define the process-relevant CH_4 flux resolution and precision requirements by characterizing the variability of wetland CH_4 emission controls using several observation-based hydrological and carbon datasets (section 2.1). We then simulate atmospheric CH_4 measurements throughout the Amazon basin for a range of low-earth orbit and geo-stationary orbit satellite OS (section 2.2), and we derive the corresponding CH_4 flux uncertainty using an idealized atmospheric inversion (section 2.3). Based on our results, we establish the OS requirements and discuss the potential of future OS to resolve Amazon wetland CH_4 emission processes (section 3). We conclude our paper in section 4.

2. Methods

We construct an Observing System Simulation Experiment (OSSE) dedicated to characterizing the spaceborne OS needed to resolve the processes controlling CH_4 fluxes from Amazon basin. Our OSSE involves the following 3 steps: we (1) characterize the variability of wetland CH_4 process controls; (2) define CH_4 flux precision requirements; and (3) define the atmospheric CH_4 concentration OS requirements (see Figure 2). We conduct our OSSE analysis using Moderate Resolution Imaging Spectroradiometer (MODIS) cloud cover and an atmospheric transport model. We focus our analysis on March 2007: March corresponds to the wet season across most of the Amazon basin, and all temporally-resolved carbon and hydrological observations chosen for this study overlap in 2007.

2.1 Wetland process controls

Wetland CH_4 emissions are controlled by a range of biogeochemical processes: inundation is likely to be a first order control of wetland emissions, as soil CH_4 production largely occurs in oxygen-depleted soils (Whalen et al., 2005). However, extensive studies of wetland CH_4 emissions suggest that inundation is not the sole determinant of spatial and temporal CH_4 emission dynamics. CH_4 can be transferred directly into the atmosphere via macrophytes, thus circumventing the aerobic soil

Atmos. Chem. Phys. Discuss., doi:10.5194/acp-2016-325, 2016
Manuscript under review for journal Atmos. Chem. Phys.
Published: 27 April 2016

layer (Whalen et al., 2005). Water-body depth (Mitsch et al., 2010), type (Devol et al., 1990) together with aquatic macrophyte density (Laanbroek 2010) can affect the proportion of wetland CH_4 transferred to the atmosphere.

Carbon (C) availability is also a determinant of wetland CH_4 emissions. Methanogen-available C turnover rates (Miyajima et al., 1997), composition (Wania et al., 2010), temporal dynamics (Bloom et al., 2012) and C stocks together drive spatial and temporal variability of carbon limitation on CH_4 production in wetlands. C cycle state variables, including the spatial variability of total biomass (Saatchi et al., 2011; Baccini et al., 2012) and soil carbon (Hiederer and Köchy, 2011) vary at <1000km scales. Methanogen-available C sources – such as gross primary production (GPP) and leaf litter –vary substantially at monthly timescales in the wet tropics (Beer et al., 2010; Chave et al., 2010; Caldararu et al., 2012). In the next section, we establish the flux resolution and precision requirements based on the variability of potential tropical wetland CH_4 emissions process controls, namely carbon uptake, live biomass and dead organic matter stocks, inundation and precipitation.

2.2 Wetland CH_4 flux requirements

Quantitative knowledge on regional processes controls on wetland CH_4 production can be obtained by assimilating retrieved CH_4 fluxes into diagnostic models using model-data fusion techniques (Fox et al., 2009; Bloom et al., 2012) or by confronting model ensembles (Melton et al., 2013) with retrieved CH_4 fluxes. Here, our aim is to provide a first order, model-independent characterization of wetland CH_4 flux retrieval requirements by quantifying basin-wide variations and co-variations in carbon and hydrological processes. By resolving wetland CH_4 fluxes at a relevant precision and resolution, the formulation and testing of wetland CH_4 emissions hypotheses can be achieved.

We use carbon stocks and fluxes as proxies for variation in C availability for methanogenesis. We characterize the spatial variability of carbon uptake based on the Jung et al., 2009 eddy-covariance based monthly 0.5° × 0.5° GPP product, and monthly 0.5° × 0.5° solar-induced fluorescence retrieved from the Global Ozone Monitoring Experiment (GOME-2)

Atmos. Chem. Phys. Discuss., doi:10.5194/acp-2016-325, 2016
Manuscript under review for journal Atmos. Chem. Phys.
Published: 27 April 2016

Atmospheric Chemistry and Physics Discussions

measurements (Joiner et al., 2013). We use the Saatchi et al., (2011) biomass map and the Hiederer and Köchy, (2011) live biomass and dead organic matter carbon stocks. We define the spatial variability of hydrological controls over methane flux based on two inundation fraction datasets (Prigent et al., 2012; Schroeder et al., 2015) and the NASA Tropical Rainfall Measuring Mission (TRMM; Huffman et al., 2007) precipitation retrievals for March 2007.

The spatial auto-correlation coefficients (Moran's I) of the seven limiting process variables indicate coherent spatial structures spanning up to 300km – 500km (Figure 3): process variables exhibit high auto-correlation at a 1° × 1° resolution (L ~ 111km), and no significant spatial correlation at 5° × 5° (L ~ 555km). We find that carbon and hydrological process variables exhibit contrasting spatial features at 3° × 3°: the cross-correlation (Pearson's r^2) of carbon and hydrological variables is <0.7 (Figure A1). Based on the process variable correlations, wetland CH_4 fluxes at L > 300km may provide insufficient information to distinguish between key wetland CH_4 process controls. We therefore expect that wetland CH_4 flux estimates at L≤300km will be critical for quantifying carbon and water process controls on wetland CH_4 emissions.

Throughout 2007, median monthly GPP variability ranges from 5% to 11% of mean GPP, and median monthly inundation variability ranges from 28% to 66%. A 25% CH_4 flux precision would permit the distinction between carbon and water as the dominant control on the temporal variability of CH_4 emissions. We set the absolute CH_4 flux precision requirement at 3 mg CH_4 m^{-2} day^{-1}; this corresponds to 25% of the Melack et al., (2004) annual Amazon-wide wetland CH_4 emission estimate (29.3 Tg CH_4 yr^{-1}, equivalent to 12 mg m^{-2} day^{-1} across 668 Mha). A monthly temporal resolution also adequately captures the seasonal variations and extremes in hydrological processes (Prigent et al., 2012; Marengo et al., 2013) and carbon processes (Chave et al., 2010; Lee et al., 2013). Given the spatial and temporal variability of potential hydrological and carbon controls, we define the following targets for wetland CH_4 flux retrievals:

- CH_4 flux spatial resolution = 300km
- CH_4 flux precision: = 3 mg CH_4 m^{-2} day^{-1}
- CH_4 flux temporal resolution: monthly

Atmos. Chem. Phys. Discuss., doi:10.5194/acp-2016-325, 2016
Manuscript under review for journal Atmos. Chem. Phys.
Published: 27 April 2016

Satellite-based CH_4 flux estimates meeting the above-stated requirements will provide robust characterization of spatial variation in Amazon wetland CH_4 emissions on the scale of variation in the major carbon and water controls, allowing forcing (hydrology and carbon) and response (CH_4 flux) to be related directly. Throughout the next subsections, we characterize the required satellite column CH_4 measurements needed to resolve CH_4 flux with the above-stated requirements. To assess the sensitivity of our results to the above-mentioned requirements, we repeat our analysis for a range of CH_4 flux spatial resolution requirements (L = 150km – 990km).

2.3 CH_4 observation requirements

We define the atmospheric CH_4 observation requirements by retrieving CH_4 fluxes from a range of low-earth orbit (LEO), and geo-stationary orbit (GEO) OS simulated CH_4 retrieved concentrations, or "observations". Our approach is three-fold: (a) we simulate LEO and GEO CH_4 observations for March 2007; (b) we derive cumulative CH_4 precision at an $L \times L$ resolution, and (c) we employ an idealized inversion to simulate CH_4 flux retrieval uncertainty for March 2007 based on the cumulative CH_4 measurement precision. We note that wetland emissions are the largest and most uncertain source of CH_4 within the Amazon river basin (Wilson et al., 2016; Melton et al., 2013). We henceforth assume that the non-wetland CH_4 contribution (namely fires and anthropogenic CH_4 sources) can be relatively well characterized using ancillary datasets and global inventories (Bloom et al., 2015; Turner et al., 2015 and references therein).

LEO and GEO CH_4 observations

The advantage of LEO systems is a near-global coverage; for the TROPOMI mission CH_4 orbit and measurement parameters, this equates to a 1-day maximum re-visit period globally. While a GEO system can only view a fixed area on the globe, revisit periods can be far shorter. To relate CH_4 observation requirements to current technological capabilities, we explore six OS configurations based on LEO and GEO OS parameters used to simulate the up-coming GEOCAPE and

Atmos. Chem. Phys. Discuss., doi:10.5194/acp-2016-325, 2016
Manuscript under review for journal Atmos. Chem. Phys.
Published: 27 April 2016

Atmospheric Chemistry and Physics Discussions

TROPOMI missions' observations in North America by Wecht et al., (2014) (Table 1). We note that, for regional CH_4 emission estimates, the GEO OS configurations are expected outperform LEO due to a larger data volume: the fixed viewing area permits multiple re-visits per day (Wecht et al., 2014), and the smaller GEO footprint size typically leads to lower cloud-contamination (Crisp et al., 2004). Our aim here is not to compare CH_4 emission estimates from LEO and GEO CH_4 retrievals. Rather, our aim is to determine whether CH_4 emission estimates from a range of LEO and GEO OS configurations are able meet the wetland process requirements outlined in section 2.1.

Cloud cover is a major limiting factor in Amazon basin trace-gas retrievals. Mean March 2007 cloud cover is 89% – ranging from 38% to 98% at a 1° × 1° resolution – throughout the Amazon river basin (based on MODIS cloud-cover data, Figure B1). We quantify the data-rejection due to cloud cover based on 1km March 2007 MODIS cloud cover data: any cloud-contaminated 3km×3km (GEO) or 7km×7km (LEO) CH_4 measurement footprints are rejected, i.e. all accepted observations are 100% cloud-free.

Densely cloud-covered areas spatially coincide with high inundation (Prigent et al., 2012) and high biomass density (Saatchi et al., 2011), which potentially correspond to areas with elevated wetland CH_4 fluxes. To assess the relative importance of CH_4 measurement density in high cloud-cover areas, we test two additional geo-stationary configurations: "GEO-Z1" carries out two visits per day and 6 visits per day in the top 50% cloudiest areas; "GEO-Z2" carries out two visits per day and 10 visits per day in the top 25% cloudiest areas (we note that these two OS would require targeting capabilities to optimize the sampling strategy over the cloudiest area of the basin). We further explore OS space by testing LEO with a $\sqrt{2}$ precision enhancement ("LEO+") and GEO with 8 visits per day instead of 4 ("GEO×2").

Cumulative CH_4 measurement precision

Atmos. Chem. Phys. Discuss., doi:10.5194/acp-2016-325, 2016
Manuscript under review for journal Atmos. Chem. Phys.
Published: 27 April 2016

Atmospheric Chemistry and Physics Discussions

For each OS ω ("GEO","LEO", etc.), $\mathbf{O}^{\{L,\omega\}}$ is the cumulative CH_4 measurement precision at a $L \times L$ resolution. $\mathbf{O}^{\{L,\omega\}}$ is an $N \times 1$ array, where N is the number of Amazon river basin grid-cells at resolution $L \times L$. We derive the cumulative atmospheric CH_4 precision within each $L \times L$ grid-cell i, $O_i^{\{L,\omega\}}$ as follows:

$$O_i^{\{L,\omega\}} = \frac{\sigma_\omega}{\sqrt{a\,\phi_i^{\{\omega\}}\,n^{\{\omega\}}\,L^2}} \qquad (1)$$

where σ_ω is the single observation precision (table 1), $\phi_i^{\{\omega\}}$ is the cloud fraction at location i, $n^{\{\omega\}}$ is the number of observations per km^2 per month for OS ω (based on Table 1 values), and a the fraction of accepted cloud-free CH_4 column retrievals (set to $a = 0.5$); The derivation of $\phi_i^{\{\omega\}}$ is based on MODIS 1-km cloud cover data over the Amazon river basin in March and September 2007 (Appendix B). The square of the denominator in (1) corresponds to the number of atmospheric column CH_4 measurements per $L \times L$ grid-cell. For all OS, $n^{\{\omega\}}$ is calculated assuming continuous basin-wide coverage at the single-sounding footprint resolution (see Table 1). We highlight that our formulation of cumulative CH_4 precision in equation 1 implies retrieved CH_4 errors are spatially and temporally uncorrelated.

OS retrieved CH_4 flux precision

We calculate the monthly retrieved CH_4 flux precision for OS ω at an $L \times L$ resolution – $\mathbf{F}^{\{L,\omega\}}$ –based on $\mathbf{O}^{\{L,\omega\}}$ (equation 1). $\mathbf{F}^{\{L,\omega\}}$ is a $N \times 1$ array, where N is the number of Amazon river basin grid-cells at resolution $L \times L$. To calculate $\mathbf{F}^{\{L,\omega\}}$ we simulate an ensemble of 1000 retrieved CH_4 concentrations vectors ($\mathbf{c}_{*,n}^{\{L,\omega\}}$ for n = 1 – 1000) over the Amazon river basin, where:

$$\mathbf{c}_{*,n}^{\{L,\omega\}} = \mathbf{c}^{\{L,0\}} + \mathbf{N}(0,1) \cdot \mathbf{O}^{\{L,\omega\}}; \qquad (2)$$

Atmos. Chem. Phys. Discuss., doi:10.5194/acp-2016-325, 2016
Manuscript under review for journal Atmos. Chem. Phys.
Published: 27 April 2016

Atmospheric Chemistry and Physics Discussions

$\mathbf{c}^{\{L,0\}}$ is a $N \times 1$ array of $L \times L$ gridded unperturbed CH_4 concentrations, $\mathbf{N}(0,1)$ is an $N \times 1$ array of normally distributed random numbers with mean zero and variance one. The unperturbed concentrations $\mathbf{c}^{\{L,0\}}$ are derived as:

$$\mathbf{c}^{\{L,0\}} = \mathbf{A}^{\{L\}}\mathbf{f}^{\{L,0\}}, \quad (3)$$

where $\mathbf{A}^{\{L\}}$ is the atmospheric transport operator (the $N \times N$ matrix transforming fluxes to concentrations over the Amazon river basin domain) and $\mathbf{f}^{\{L,0\}}$ is an $N \times 1$ array of unperturbed surface CH_4 fluxes (where for i=1 – N, $f_i^{\{L,0\}}$= 12 mg m^{-2} day^{-1}).

For the sake of brevity, we present a summary of $\mathbf{A}^{\{L\}}$ here, and the complete derivation of $\mathbf{A}^{\{L\}}$ in Appendix C. We use a Lagrangian Particle Dispersion Model (LPDM: Uliasz, 1994; Lauvaux and Davis, 2014) to derive an "influence function" (or "column footprint") relating satellite-retrieved atmospheric CH_4 concentrations to surface fluxes (the inverse solution of the transport from the surface to higher altitudes) at the center of the study area. We simulate 30km × 30km CH_4 transport – $\mathbf{A}^{\{30\text{km}\}}$ – by spatially translating the LPDM influence function throughout the domain. To assess the robustness of the LPDM approach, we also simulated CH_4 column mixing ratios over the Amazon river basin at 30km using the Weather Research and Forecasting model (WRF v2.5.1, Skamarock et al., 2008). The WRF model March 2007 Amazon river basin concentrations and the corresponding LPDM approximations are shown in Figure A2. Finally, we used a Monte Carlo approach to statistically construct $\mathbf{A}^{\{L\}}$ based on $\mathbf{A}^{\{30\text{km}\}}$. The LPDM, WRF and the Monte Carlo derivation of $\mathbf{A}$ are fully described in Appendix C.

For each L, we simulate the flux uncertainty based on the inverse of $\mathbf{A}^{\{L\}}$, $(\mathbf{A}^{\{L\}})^{-1}$ and simulated CH_4 concentrations vectors ($\mathbf{c}_{*,n}^{\{L,\omega\}}$, equation 2). The n^{th} retrieved flux estimate – $\mathbf{f}_{*,n}^{\{L,\omega\}}$ – is calculated as:

$$\mathbf{f}_{*,n}^{\{L,\omega\}} = (\mathbf{A}^{\{L\}})^{-1}\,\mathbf{c}_{*,n}^{\{L,\omega\}}. \quad (4)$$

Atmos. Chem. Phys. Discuss., doi:10.5194/acp-2016-325, 2016
Manuscript under review for journal Atmos. Chem. Phys.
Published: 27 April 2016

Atmospheric Chemistry and Physics Discussions

Finally, we calculate the flux precision $\mathbf{F}^{\{L,\omega\}}$ at grid-cell i as follows:

$$F_i^{\{\omega,L\}} = \frac{StDev\left(\mathbf{f}_{i,*}^{\{\omega,L\}}\right)}{f_i^{\{L,0\}}} \times 100\%. \quad (5)$$

3. Results and Discussion

Cumulative CH_4 precision for mean monthly atmospheric column CH_4 measurements is 0.11 – 1.08 ppb for the LEO OS (figure 4, left) and 0.02 – 0.28 ppb for the GEO OS (figure 4, right). The lowest CH_4 concentration precision occurs in the East and central Amazon river basin. A crucial advantage of the smaller GEO footprint is the 88-148% higher probability of cloud-free observations in the cloudiest regions of the Amazon river basin (Figure B1).

For L = 300km, median monthly retrieved CH_4 flux precision for the LEO OS (median of $\boldsymbol{F}^{\{LEO,300km\}}$) is 186% (Figure 5); increasing the single sounding retrieval precision by $\sqrt{2}$ (from 0.6ppb to 0.42ppb) for LEO observations (LEO+) reduces the retrieved flux uncertainty to 132%. This uncertainty reduction is equivalent to a second LEO visit per day (see table 1): the factor 3-to-10 lower uncertainties for cumulative GEO CH_4 concentrations (Figure 4) lead to a 30% uncertainty in the retrieved flux (Figure 5). Doubling the number of GEO visits per day (GEOx2 OS) reduces the retrieved flux uncertainty to 22%. GEO-Z1 and GEO-Z2 uncertainties (27% and 21%) are both lower than GEO. These results indicate that – despite a lower number of accepted observations – a higher observation density in the high cloud-cover areas of the Amazon river basin (and lower observation density elsewhere) can be used to reduce the retrieved CH_4 flux uncertainty without increasing the number of observations per day.

Conventional GEO and LEO observations can resolve median monthly Amazon CH_4 fluxes at a ≥750km resolution (Figure 6). However, estimates of fluxes at higher resolutions, i.e. L = 300 – 750km, show that GEO retrieved CH_4 flux uncertainty

Atmos. Chem. Phys. Discuss., doi:10.5194/acp-2016-325, 2016
Manuscript under review for journal Atmos. Chem. Phys.
Published: 27 April 2016

Atmospheric Chemistry and Physics Discussions

is consistently lower by a factor of 5 than the LEO retrieved CH_4 flux uncertainty. GEO 0 – 95th%ile of flux estimates can be resolved at <25% uncertainty for L>400km, while LEO 0 – 95th%ile of flux estimates can be resolved at <25% at L>900km.

We find that a 1 observation km^{-2} month^{-1} OS can resolve Amazon wetland CH_4 fluxes at the required precision/resolution (Figure 5). By optimizing the number of observations in densely clouded areas, OSs with a mean observation density of 0.5 observations km^{-2} month^{-1} can also retrieve fluxes at the required precision/resolution. Based on the LEO OS, we anticipate that missions similar to the ESA TROPOMI observation configuration (Wecht et al., 2014) will lead to lower-than-required information content for Amazon wetlands and are unlikely to provide sufficient observational constraints to resolve the dominant CH_4 flux processes.

In our analysis we have assumed (i) perfectly known boundary conditions, and (ii) no systematic biases in our atmospheric inversion simulation. For example, significant systematic atmospheric CH_4 retrieval and transport model biases can undermine the enhanced accuracy of geostationary OSs. A quantitative assessment of transport errors and atmospheric CH_4 bias structures should be performed to characterize the accuracy of CH_4 flux retrievals. However, GEO missions are likely to provide a higher volume of observations at the boundaries of the observation domain, relative to LEO OS: therefore, boundary conditions are likely to reinforce the potential of GEO OS compared to LEO.

Our CH_4 flux uncertainty requirement (25% or 3 mg CH_4 m^{-2} day^{-1}) is based on uniformly distributed fluxes at $L \times L$ resolution. Wetland CH_4 emission models (Melton et al., 2013) suggest major CH_4 emissions along the main stem of the Amazon river (Figure 1); if Amazon wetland CH_4 fluxes are primarily emitted from high inundation fraction areas, associated uncertainties will likely be lower (see equation 5). Prior information on the magnitude and variability of fluxes can also be introduced (e.g. in a Bayesian atmospheric transport and chemistry inversion framework) to re-assess posterior uncertainty estimates. However, as outlined in section 2.1, large unknowns preside over the processes governing the spatial and temporal variability of wetland CH_4 fluxes. Therefore, the introduction of prior spatial and temporal correlations in wetland CH_4 flux estimates would hinder the potential to resolve processes at the required spatial and temporal resolutions.

Atmos. Chem. Phys. Discuss., doi:10.5194/acp-2016-325, 2016
Manuscript under review for journal Atmos. Chem. Phys.
Published: 27 April 2016

To our knowledge, our analysis provides a first quantification of the OS requirements for confronting prior knowledge on CH_4 fluxes at a process-relevant resolution.

4. Concluding remarks

Quantitative knowledge of biogeochemical processes controlling biosphere-atmosphere greenhouse gas fluxes remains highly uncertain. Optimally designed satellite greenhouse gas observing systems can potentially resolve the processes controlling critical boreal and tropical greenhouse gas fluxes. In this study, we have characterized a satellite OS able to resolve the principal process controls on Amazon river basin wetland CH_4 emissions. Conventional low-earth orbit satellite missions will likely be unable to resolve Amazon wetland CH_4 emissions at a process-relevant scale and precision. Observation density in time and space, and its reduction by cloud cover are the major limiting factors. Increasing the number of daily CH_4 measurements in cloudy regions at the expense of other measurements can significantly reduce the retrieved CH_4 flux precision from geostationary satellite CH_4 measurements. OSSEs based on reducing process uncertainty can inform observation requirements for future greenhouse gas satellite missions in a far more targeted way than simply quantifying overall flux uncertainty reduction for a given OS.

Appendix A.

We use the Jung et al., (2009) gross primary production (GPP) dataset and Schroeder et al., (2015) MEaSUREs inundation fraction (MIA) dataset. The two datasets are aggregated at a 0.5°×0.5° resolution. The Oki and Sud (1998) river basin dataset is used to delineate Amazon river basin GPP and MIA data. For MIA, we excluded inundation within 1° of the coastline, as these areas are not representative of Amazon wetland regions. The GPP and MIA Pearson's auto-correlation coefficients are calculated at 0.5° increments in the North-South direction and the East-West direction. The mean "Carbon" and "Water" autocorrelations at 0.5° increments are shown in Figure 3a.

Atmos. Chem. Phys. Discuss., doi:10.5194/acp-2016-325, 2016
Manuscript under review for journal Atmos. Chem. Phys.
Published: 27 April 2016

Atmospheric Chemistry and Physics Discussions

Moran's I.

For each process control dataset, we derive the Moran's I spatial auto-correlation coefficient (r_{MI}) at an $L \times L$ resolution, where L = 0.5°, 1°, 1.5°, … , 10°. For every L we aggregated the dataset to $L \times L$ resolution. To determine whether the derived r_{MI} are significant relative to the null hypothesis, we repeat the Moran's I derivation 2000 times for normally distributed random numbers (in the place of the $L \times L$ gridded dataset), which together statistically represent the Moran's I distribution ($\mathbf{R}_{MI}$) for statistically insignificant spatial correlation. For r_{MI} > (<) median $\mathbf{R}_{MI}$, the r_{MI} p-value is twice the fraction of $\mathbf{R}_{MI}$ > (<) r_{MI}. We define the correlation length as $L = r_{MI}$, where r_i is the value of r at which the correlation in insignificant.

Appendix B

The MODIS cloud cover analysis was performed based on the MOD06_L2 1km cloud mask product (downloaded from modis.gsfc.nasa.gov). We consider "probably cloudy" and "cloudy" 1km × 1km pixel flags as cloud-covered areas (CC = 1), and the remaining pixel flag categories ("probably clear" and "clear") as cloud-free areas (CC=0). We aggregate the 1km data to *N*km × *N*km (*N* is the OS footprint resolution; GEO N = 3km; LEO N = 7km; see Table 1) to calculate the cloud-cover fraction for all *N*km × *N*km areas within each MODIS cloud cover scene. The monthly mean effective cloud cover fraction $f_{(\omega,i)}$ (see equation 1) is calculated by deriving the ratio of cloud-free to total *N*km × *N*km areas within each 30km × 30km area. A regional summary of the observation yields (% of cloud-free *N*km × *N*km areas) for a range of footprint resolutions (*N* = 1 – 10km) is shown in Figure B1.

Appendix C

Atmospheric transport operator

Atmos. Chem. Phys. Discuss., doi:10.5194/acp-2016-325, 2016
Manuscript under review for journal Atmos. Chem. Phys.
Published: 27 April 2016

Atmospheric Chemistry and Physics Discussions

For L = 150km - 990km, we derive the $N \times N$ atmospheric transport operator $\mathbf{A}^{\{L\}}$ for $L \times L$ resolution fluxes based on N random CH_4 flux vectors ($\mathbf{f}'^{\{L\}}_{*,n}$ for n = 1 – N) and their corresponding concentrations ($\mathbf{c}'^{\{L\}}_{*,n}$ for n = 1 – N), where,

$$\mathbf{A}^{\{L\}} = \left(\mathbf{f}'^{\{L\}}\right)^{-1}\mathbf{c}'^{\{L\}}. \qquad \text{(C1)}$$

Random CH_4 fluxes at grid-cell i are derived as $f'^{\{L\}}_{i,n} = \mathrm{R}(0,1)$, where R(0,1) is a random number sampled from a normal distribution with mean zero and variance 1. Atmospheric concentrations are firstly simulated at resolution L_0 = 30km; the fluxes $\mathbf{f}'^{\{L\}}_{*,n}$ are downscaled to $L_0 \times L_0$ resolution ($\mathbf{f}'^{\{L_0\}}_{*,n}$). For each 30km × 30km grid-cell i, the mean atmospheric CH_4 concentration $c^{\{L_0\}}_i$ is calculated as

$$c'^{\{L_0\}}_{i,n} = \mathbf{I}_i\mathbf{f}'^{\{L_0\}}_{*,n} \qquad \text{(C2)}$$

where $\mathbf{f}^{\{L_0\}}_{*,n}$ is the N × 1 array of CH_4 fluxes, $\mathbf{I}_i$ is the N × 1 influence function array for grid-cell i. We derive $\mathbf{I}_i$ using a Lagrangian Particle Dispersion Model (LPDM, Uliasz, 1994). The influence function derivation (i.e. the column sensitivity to the surface fluxes) is described in Lauvaux and Davis (2014). The influence function was computed for an averaged column observation in the model of the simulation domain, for every hour of March 2007. The inverse calculation of surface fluxes requires the use of the adjoint of the transport at the mesoscale (~2000km). Here, we only simulated the fraction of the column influenced by surface fluxes. We assume boundary conditions are well constrained by satellite and surface network measurements: therefore, only the first 6km of the column was described by the particles released backward in the model.

To simulate total column CH_4 retrieval influence functions, we incorporate a mean GOSAT CH_4 retrieved averaging kernel (Parker et al., 2011) for the Amazon river basin region (Figure A1). To minimize the computational cost of simulating atmospheric transport, we (i) derive the influence function for the center of the domain ($\mathbf{I}_0$, Lat = 4.9°S and Lon = 63.8°W), and (ii) we derive $\mathbf{I}_i$ by spatially translating $\mathbf{I}_0$ to gridcell i latitude and longitude coordinates. Finally, we derive mean $L \times L$

Atmos. Chem. Phys. Discuss., doi:10.5194/acp-2016-325, 2016
Manuscript under review for journal Atmos. Chem. Phys.
Published: 27 April 2016

Atmospheric Chemistry and Physics Discussions

resolution concentrations used in equation C1, ($\mathbf{c}_{*,n}^{\prime\{L\}}$), based on the spatial aggregation of $L_0 \times L_0$ resolution concentrations $\mathbf{c}_{*,n}^{\prime\{L_0\}}$.

To assess the viability of our approach, we simulate March 2007 $L_0 \times L_0$ atmospheric concentrations – based on $\mathbf{f}^{\{L_0,0\}}$, where for i=1 – N, $f_i^{\{L_0,0\}}$= 12 mg m^{-2} day^{-1} – throughout the Amazon river basin domain using (a) equation C2, and (b) WRF CH_4 atmospheric transport model. In the WRF model, $\mathbf{f}^{\{L_0,0\}}$ was coupled to the atmospheric model through the chemistry modules (WRF-Chem) for passive tracers, as described in Lauvaux et al. (2012). The physics configuration of the model used Mellor-Yamada-Nakanishi-Niino scheme for the Planetary Boundary Layer (Nakanishi and Niino, 2004), the NOAH land surface model (Pan and Mahrt, 1987), the WSM-5 microphysics scheme (Hong et al., 2004), and the Kin-Fritsch cumulus parameterization (Kain, 2004). The meteorological driver data from the Global Forecasting System (FNL) analysis products at 1° × 1° resolution was used at the boundaries of the simulation domain. The simulation domain spans 120x100 $L_0 \times L_0$ grid-points, and 60 vertical levels to describe the atmospheric column up to 50 hPa. The atmospheric column was extracted from the surface to the top of the modeled atmosphere, which represents about 90% of the total air mass. A dilution factor of 0.9 was used to compensate for the partial model column.

The LPDM approach emulates the large-scale WRF CH_4 enhancement (r^2 = 0.85 see Figure C1); the smoothing effect is due to the use of a single footprint throughout the entire domain. Mean CH_4 concentrations based on our approach (equation C2) and WRF are 15.23ppb and 17.42ppb respectively.

Acknowledgments

Part of this research was carried out at the Jet Propulsion Laboratory, California Institute of Technology, under a contract with the National Aeronautics and Space Administration. Inundation datasets are available at noaacrest.org/rscg/ and wetlands.jpl.nasa.gov. TRMM data is available at mirador.gsfc.nasa.gov. The gross primary production dataset was obtained from bgc-jena.mpg.de. The soil carbon dataset is available at esdac.jrc.ec.europa.eu.

Atmos. Chem. Phys. Discuss., doi:10.5194/acp-2016-325, 2016
Manuscript under review for journal Atmos. Chem. Phys.
Published: 27 April 2016

Atmospheric Chemistry and Physics Discussions

References

Andrews, A. E., Kofler, J. D., Trudeau, M. E., Williams, J. C., Neff, D. H., Masarie, K. A., Chao, D. Y., Kitzis, D. R., Novelli, P. C., Zhao, C. L., Dlugokencky, E. J., Lang, P. M., Crotwell, M. J., Fischer, M. L., Parker, M. J., Lee, J. T., Baumann, D. D., Desai, A. R., Stanier, C. O., De Wekker, S. F. J., Wolfe, D. E., Munger, J. W., and Tans, P. P.: CO2, CO, and CH4 measurements from tall towers in the NOAA Earth System Research Laboratory's Global Greenhouse Gas Reference Network: instrumentation, uncertainty analysis, and recommendations for future high-accuracy greenhouse gas monitoring efforts, *Atmos. Meas. Tech.*, 7, 647–687, doi:10.5194/amt-7-647-2014, 2014.

Baccini, A., Goetz, S. J., Walker, W. S., Laporte, N. T., Sun, M., Sulla-Menashe, D., Hackler, J., Beck, P. S. A., Dubayah, R., Friedl, M. A., Samanta, S., and Houghton, R. A.: Estimated carbon dioxide emissions from tropical deforestation improved by carbon-density maps, *Nat. Climate Change*, 2, 182– 185; doi:10.1038/nclimate1354, 2012.

Bacastow, R. B., Adams, J. A., Keeling, C. D., Moss, D. J., Whorf, T. P., and Wong, C. S.: Atmospheric carbon dioxide, the Southern Oscillation, and the weak 1975 El Niño, *Science*, 210, 66–68, doi:10.1126/science.210.4465.66, 1980.

Basso, L. S., Gatti, L. V., Gloor, M., Miller, J. B., Domingues, L. G., Correia, C. S., and Borges, V. F.: Seasonality and interannual variability of CH_4 fluxes from the eastern Amazon Basin inferred from atmospheric mole fraction profiles. *J Geophys Res-Atmos*, 121, 168–184, doi: 10.1002/2015JD023874, 2016.

Beer, C., Reichstein, M., Tomelleri, E., Ciais, P., Jung, M., Carvalhais, N., Rodenbeck, C., Arain, M. A., Baldocchi, D., Bonan, G. B., Bondeau, A., Cescatti, A., Lasslop, G., Lindroth, A., Lomas, M., Luyssaert, S., Margolis, H., Oleson, K. W., Roupsard, O., Veenendaal, E., Viovy, N., Williams, C., Woodward, F. I., and Papale, D.: Terrestrial Gross Carbon Dioxide Uptake: Global Distribution and Covariation with Climate, *Science,* 329, 834– 838, doi:10.1126/Science.1184984, 2010.

Bergamaschi, P., Houweling, S., Segers, A., Krol, M., Frankenberg, C., Scheepmaker, R. A., Dlugokencky, E., Wofsy, S. C., Kort, E. A., Sweeney, C., Schuck, T., Brenninkmeijer, C., Chen, H., Beck, V., and Gerbig, C.: Atmospheric CH_4 in the first decade of the 21st century: Inverse modeling analysis using SCIAMACHY satellite retrievals and NOAA surface measurements, *J. Geophys. Res.*, 118, 7350–7369, doi:10.1002/jgrd.50480, 2013.

Bloom, A. A., Palmer, P. I., Fraser, A., Reay, D. S., and Frankenberg, C.: Large-Scale Controls of Methanogenesis Inferred from Methane and Gravity Spaceborne Data, *Science*, 327, 322–325, doi:10.1126/Science.1175176, 2010.

Bloom, A. A., Palmer, P. I., Fraser, A., and Reay, D. S.: Seasonal variability of tropical wetland CH_4 emissions: the role of the methanogen-available carbon pool, *Biogeosciences*, 9, 2821– 2830, doi:10.5194/bg-9-2821-2012, 2012.

Bloom, A. A., Worden, J., Jiang, Z., Worden, H., Kurosu, T., Frankenberg, C., and Schimel, D.: Remote sensing constraints on South America fire traits by Bayesian fusion of atmospheric and1140 surface data, *Geophys. Res. Lett.*, 42, 1268–1274, doi: 10.1002/2014GL062584, 2015.

Bloom, A. A., Exbrayat, J.-F., van der Velde, I. R., Feng, L., Williams., M. The decadal state of the terrestrial carbon cycle: Global retrievals of terrestrial carbon allocation, pools, and residence times. *P. Natl. Acad. Sci.*, 113, 1285–1290, doi: 10.1073/pnas.1515160113, 2016.

Bousquet, P., Ringeval, B., Pison, I., Dlugokencky, E. J., Brunke, E.-G., Carouge, C., Chevallier, F., Fortems-Cheiney, A., Frankenberg, C., Hauglustaine, D. A., Krummel, P. B., Langenfelds, R. L., Ramonet, M., Schmidt, M., Steele, L. P., Szopa, S., Yver, C., Viovy, N., and Ciais, P.: Source attribution of the changes in atmospheric methane for 2006–2008, *Atmos. Chem. Phys.*, 11, 3689-3700, doi:10.5194/acp-11-3689-2011, 2011.

Bousserez, N., Henze, D. K., Rooney, B., Perkins, A., Wecht, K. J., Turner, A. J., Natraj, V., and Worden, J. R.: Constraints on methane emissions in North America from future geostationary remote sensing measurements, *Atmos. Chem. Phys. Discuss.*, 15, 19017-19044, doi:10.5194/acpd-15-19017-2015, 2015.

Braswell, B. H., Schimel, D. S., Linder, E., & Moore, B. I. I. I.: The response of global terrestrial ecosystems to interannual temperature variability. *Science*, 278, 870-873, doi: 10.1126/science.278.5339.870, 1997.

Butz, A., Guerlet, S., Hasekamp, O., Schepers, D., Galli, A., Aben, I., Frankenberg, C., Hartmann, J.-M., Tran, H., Kuze, A., Keppel-Aleks, G., Toon, G., Wunch, D., Wennberg, P., Deutscher, N., Griffith, D., Macatangay, R., Messerschmidt, J., Notholt, J., and Warneke, T.: Toward accurate CO_2 and CH_4 observations from GOSAT, *Geophys. Res. Lett.*, 38, L14812, doi:10.1029/2011GL047888, 2011.

Butz, A., Galli, A., Hasekamp, O., Landgraf, J., Tol, P., and Aben, I.: TROPOMI aboard Sentinel-5 Precursor: Prospective performance of CH_4 retrievals for aerosol and cirrus loaded atmospheres, *Remote Sens. Environ.*, 120, 267–276, doi:10.1016/j.rse.2011.05.030, 2012.

Caldararu, S., Palmer, P. I., and Purves, D. W.: Inferring Amazon leaf demography from satellite observations of leaf area index, *Biogeosciences*, 9, 1389–1404, doi:10.5194/bg-9-1389- 2012, 2012.

Chave, J., Navarrete, D., Almeida, S., Álvarez, E., Aragão, L.E.O. C., Bonal, D., Châtelet, P., Silva-Espejo, J. E., Goret, J.-Y., von Hildebrand, P., Jiménez, E., Patiño, S. , Peñuela, M. C., Phillips, O. L., Stevenson, P., and Malhi, Y.: Regional and seasonal pat- terns of litterfall in tropical South America, *Biogeosciences*, 7, 43–55, doi:10.5194/bg-7-43-2010, 2010.

Chen, Y., Randerson, J. T., and Morton, C. D.: Tropical North Atlantic ocean-atmosphere interactions synchronize forest carbon losses from hurricanes and Amazon fires. *Geophysical Research Letters*, 42: 6462-6470, doi: 10.1002/2015GL064505, 2015.

Cox, P. M., Pearson, D., Booth, B. B., Friedlingstein, P., Huntingford, C., Jones, C. D., and Luke, C. M.: Sensitivity of tropical carbon to climate change constrained by carbon dioxide variability, *Nature*, 494, 341–344, doi:10.1038/nature11882, 2013.

Crevoisier, C., Nobileau, D., Fiore, A. M., Armante, R., Chédin, A., and Scott, N. A.: Tropospheric methane in the tropics – first year from IASI hyperspectral infrared observations, *Atmos. Chem. Phys.*, 9, 6337-6350, doi:10.5194/acp-9-6337-2009, 2009.

Crisp, D., Atlas, R. M., Breon, F.-M., Brown, L. R., Burrows, J. P., Ciais, P., Connor, B. J., Doney, S. C., Fung, I. Y., Jacob, D. J., Miller, C. E., O'Brien, D., Pawson, S., Randerson, J. T., Rayner, P., Salawitch, R. J., Sander, S. P., Sen, B., Stephens, G. L., Tans, P. P., Toon, G. C., Wennberg, P. O., Wofsy, S. C., Yung, Y. L., Kuang, Z., Chudasama, B., Sprague, G., Weiss, B., Pollock, R., Kenyon, D., and Schroll, S.: The Orbiting Carbon Observatory (OCO) mission, *Adv. Space Res.*, 34, 700–709, doi:10.1016/j.asr.2003.08.062, 2004.

Devol, A. H., Richey, J. E., Forsberg, B. R., and Martinelli, L. A.: Seasonal dynamics in methane emissions from the Amazon River floodplain to the troposphere, *J. Geophys. Res.*, 95, 16417–16426, doi:10.1029/JD095iD10p16417, 1990.

Fox, A., Williams, M., Richardson, A. D., Cameron, D., Gove, J. H., Quaife, T., Ricciuto, D., Reichstein, M., Tomelleri, E., Trudinger, C. M., and Van Wijk, M. T.: The REFLEX project: Comparing different algorithms and implementations for the inversion of a terrestrial ecosystem model against eddy covariance data, *Agr. Forest Meteorol.*, 149, 1597–1615, doi:10.1016/j.agrformet.2009.05.002, 2009.

Frankenberg, C., Bergamaschi, P., Butz, A., Houweling, S., Meirink, J. F., Notholt, J., Petersen, A. K., Schrijver, H., Warneke, T., and Aben, I.: Tropical methane emissions: A re- vised view from SCIAMACHY onboard ENVISAT, *Geophys. Res. Lett.*, 35, L15811, doi:10.1029/2008GL034300, 2008.

Franklin, J., Serra-Diaz, J. M., Syphard, A. D., and Regan, H. M.: Global change and terrestrial plant community dynamics, *P. Natl. Acad. Sci.*, 113, 3725–3734, doi: 10.1073/pnas.1519911113, 2016

Fung, I., John, J., Lerner, J., Matthews, E., Prather, M., Steele, L. P., and Fraser, P. J.: Three-dimensional model synthesis of the global methane cycle, *J. Geophys. Res.*, 96, 13033–13065, doi:10.1029/91JD01247, 1991.

Friedlingstein, P., Meinshausen, M., Arora, V. K., Jones, C. D., Anav, A., Liddicoat, S. K., and Knutti, R.: Uncertainties in CMIP5 climate projections due to carbon cycle feedbacks, *J. Climate*, 27, 511–526, doi:10.1175/JCLI-D-12-00579.1, 2013.

Gurney, K. R., Baker, D., Rayner, P., Denning, S., Law, R., Bousquet, P., Bruhwiler, L., Chen, Y. H., Ciais, P., Fung, I., Heimann, M., John, J., Maki, T., Maksyutov, S., Peylin, P., Prather, M., Pak, B., and S. Taguchi, S.: Interannual variations in continental-scale net carbon exchange and sensitivity to observing networks estimated from atmospheric CO_2 inversions for the period 1980–2005, *Global Biogeochem. Cy.*, 22, GB3025, doi:10.1029/2007GB003082, 2008.

Hong, S., Dudhia, J., and Chen, S.: A revised approach to ice microphysical processes for the bulk parameterization of clouds and precipitation, *Mon. Weather Rev.*, 132, 103–120, 2004.

Hiederer, R. and M. Köchy: Global soil organic carbon estimates and the harmonized world soil database, EUR, 79, 25225, doi:10.2788/13267, 2011.

Huffman, G. J., Bolvin, D. T., Nelkin, E. J., Wolff, D. B., Adler, R. F., Gu, G., Hong, Y., Bowman, K. P., and Stocker, E. F.: The TRMM Multisatellite Precipitation Analysis (TMPA): Quasi-global, multiyear, combined-sensor precipitation estimates at fine scales, *J. Hydrometeorol.*, 8, 38–55, doi:10.1175/JHM560.1, 2007.

Huntzinger, D. N., Post, W. M., Wei, Y., Michalak, A. M., West, T. O., Jacobson, A. R., Baker, I. T., Chen, J. M., Davis, K. J., Hayes, D. J., Hoffman, F. M., Jain, A. K., Liu, S., McGuire, A. D., Neilson, R. P., Potter, C., Poulter, B., Price, D., Raczka, B. M., Tian, H. Q., Thornton, P., Tomelleri, E., Viovy, N., Xiao, J., Yuan, W., Zeng, N., Zhao, M., and Cook, R.: North American Carbon Project (NACP) Regional Interim Synthesis: Terrestrial Biospheric Model Intercomparison, *Ecol. Model.*, 224, 144–157, doi:10.1016/j.ecolmodel.2012.02.004, 2012.

Joiner, J., Guanter, L., Lindstrot, R., Voigt, M., Vasilkov, A. P., Middleton, E. M., Huemmrich, K. F., Yoshida, Y., and Frankenberg, C.: Global monitoring of terrestrial chlorophyll fluorescence from moderate-spectral-resolution near-infrared satellite mea- surements: methodology, simulations, and application to GOME- 2, *Atmos. Meas. Tech.*, 6, 2803–2823, doi:10.5194/amt-6-2803- 2013, 2013.

Jung, M., Reichstein, M., and Bondeau, A.: Towards global empirical upscaling of FLUXNET eddy covariance observations: validation of a model tree ensemble approach using a biosphere model, *Biogeosciences*, 6, 2001-2013, doi:10.5194/bg-6-2001-2009, 2009.

Laanbroek, H. J.: Methane emission from natural wetlands: interplay between emergent macrophytes and soil microbial processes, A mini-review, *Ann. Bot.-London*, 105, 141–153, 2010.

Kain, J. S.: The Kain–Fritsch Convective Parameterization: An Update, *J. Appl. Meteorol.*, 43, 170–181, doi:10.1175/1520-0450(2004)043<0170:TKCPAU>2.0.CO;2, 2004.

King, A. W., Andres, R. J., Davis, K. J., Hafer, M., Hayes, D. J., Huntzinger, D. N., de Jong, B., Kurz, W. A., McGuire, A. D., Vargas, R., Wei, Y., West, T. O., and Woodall, C. W.: North America's net terrestrial CO2 exchange with the atmosphere 1990–2009, *Biogeosciences*, 12, 399-414, doi:10.5194/bg-12-399-2015, 2015.

Kirschke, S., Bousquet, P., Ciais, P., Saunois, M., Canadell, J. G., Dlugokencky, E. J., Bergamaschi, P., Bergmann, D., Blake, D. R., Bruhwiler, L., Cameron-Smith, P., Castaldi, S., Chevallier, F., Feng, L., Fraser, A., Heimann, M., Hodson, E. L., Houweling, S., Josse, B., Fraser, P. J., Krummel, P. B., Lamarque, J.- F., Langenfelds, R. L., Le Quéré, C., Naik, V., O'Doherty, S., Palmer, P. I., Pison, I., Plummer, D., Poulter, B., Prinn, R. G., Rigby, M., Ringeval, B., Santini, M., Schmidt, M., Shindell, D. T., Simpson, I. J., Spahni, R., Steele, L. P., Strode, S. A., Sudo, K., Szopa, S., van der Werf, G. R., Voulgarakis, A., van Weele, M., Weiss, R. F., Williams, J. E., and Zeng, G.: Three decades of global methane sources and sinks, *Nat. Geosci.*, 6, 813–823, doi:10.1038/ngeo1955, 2013.

Lauvaux, T., Schuh, A. E., Uliasz, M., Richardson, S., Miles, N., Andrews, A. E., Sweeney, C., Diaz, L. I., Martins, D., Shepson, P. B., and Davis, K. J.: Constraining the CO2 budget of the corn belt: exploring uncertainties from the assumptions in a mesoscale inverse system, *Atmos. Chem. Phys.*, 12, 337-354, doi:10.5194/acp-12-337-2012, 2012.

Lauvaux, T. and Davis, K. J.: Planetary boundary layer errors in mesoscale inversions of column-integrated CO_2 measurements, *J. Geophys. Res.-Atmos.*, 119, 490–508, doi:10.1002/2013jd020175, 2014.

Lee, J.-E., Frankenberg, C., van der Tol, C., Berry, J. A., Guanter, L., Boyce, C. K., Fisher, J. B., Morrow, E., Worden, J. R., Asefi, S., Badgley, G., and Saatchi, S.: Forest productivity and water stress in Amazonia: observations from GOSAT chlorophyll fluorescence, *Proc. R. Soc. B*, 280, 20130171, doi:10.1098/rspb.2013.0171, 2013.

Marengo, J. A., Alves, L. M., Soares, W. R., Rodriguez, W. R., Camargo, H., Paredes Riveros, M., and Diaz Pabló, A.: Two Contrasting Severe Seasonal Extremes in Tropical South America in 2012: Flood in Amazonia and Drought in Northeast Brazil. J. Climate, 26, 9137–9154, doi: 10.1175/JCLI-D-12-00642.1, 2013.

Melack, J. M., Hess, L. L., Gastil, M., Forsberg, B. R., Hamilton, S. K., Lima, I. B. T., and Nova, E. M. L. M.: Regionalization of methane emissions in the Amazon basin with microwave remote sensing, *Global Change Biol.*, 10, 530–544, 2004.

Melton, J. R., Wania, R., Hodson, E. L., Poulter, B., Ringeval, B., Spahni, R., Bohn, T., Avis, C. A., Beerling, D. J., Chen, G., Eliseev, A. V., Denisov, S. N., Hopcroft, P. O., Lettenmaier, D. P., Riley, W. J., Singarayer, J. S., Subin, Z. M., Tian, H., Zürcher, S., Brovkin, V., van Bodegom, P. M., Kleinen, T., Yu, Z. C., and Kaplan, J. O.: Present state of global wetland extent and wetland methane modelling: conclusions from a model inter-comparison project (WETCHIMP), *Biogeosciences*, 10, 753-788, doi:10.5194/bg-10-753-2013, 2013.

Mitsch, W., Nahlik, A., Wolski, P., Bernal, B., Zhang, L., and Ram- berg, L.: Tropical wetlands: seasonal hydrologic pulsing, carbon sequestration, and methane emissions, *Wetlands Ecol. Manage.*, 18, 573–586, doi:10.1007/s11273-009-9164-4, 2010.

Miyajima, T., Wada, E., Hanba, Y. T., and Vijarnsorn, P.: Anaerobic mineralization of indigenous organic matters and methanogene- sis in tropical wetland soils, *Geochimica et Cosmochimica Acta*, 61, 3739–3751, doi:10.1016/S0016-7037(97)00189-0, 1997.

Myhre, G., Shindell, D., Bréon, F.-M., Collins, W., Fuglestvedt, J., Huang, J., Koch, D., Lamarque, J.-F., Lee, D., Mendoza, B., Nakajima, T., Robock, A., Stephens, G., Takemura, T., and Zhang, H.: Anthropogenic and Natural Radiative Forcing, *in: Climate Change 2013: The Physical Science Basis. Contribution of Working Group I to the Fifth Assessment Report of the*

Intergovernmental Panel on Climate Change, edited by: Stocker, T. F., Qin, D., Plattner, G.-K., Tignor, M., Allen, S. K., Boschung, J., Nauels, A., Xia, Y., Bex, V., and Midgley, P. M., Cambridge University Press, Cambridge, United Kingdom and New York, NY, USA, 2013.

Nakanishi, M. and Niino, H.: An improved Mellor-Yamada level-3 model with condensation physics: its design and verification, *Bound.-Lay. Meteorol.*, 112, 1–31, doi:10.1023/B:BOUN.0000020164.04146.98, 2004.

Oki, T. and Sud, Y. C.: Design of Total Runoff Integrating Pathways (TRIP) – A global river channel network, *Earth Interact.,* 2, 1–37, 1998.

Pan, H-L., and Mahrt, L.: Interaction between soil hydrology and boundary-layer development. *Bound.-Lay. Meteorol.* 38, 185-202, doi:10.1007/BF00121563, 1987.

Parker, R., Boesch, H., Cogan, A., Fraser, A., Feng, L., Palmer, P. I., Messerschmidt, J., Deutscher, N., Griffith, D. W. T., Notholt, J., Wennberg, P. O., and Wunch, D.: Methane observations from the greenhouse gases observing satellite: comparison to ground-based TCCON data and model calculations, *Geophys. Res. Lett.*, 38, L15807, doi:10.1029/2011GL047871, 2011.

Peylin, P., Law, R. M., Gurney, K. R., Chevallier, F., Jacobson, A. R., Maki, T., Niwa, Y., Patra, P. K., Peters, W., Rayner, P. J., Rödenbeck, C., van der Laan-Luijkx, I. T., and Zhang, X.: Global atmospheric carbon budget: results from an ensemble of atmospheric CO_2 inversions, *Biogeosciences*, 10, 6699-6720, doi:10.5194/bg-10-6699-2013, 2013.

Pison, I., Ringeval, B., Bousquet, P., Prigent, C., and Papa, F.: Stable atmospheric methane in the 2000s: key-role of emissions from natural wetlands, *Atmos. Chem. Phys.*, 13, 11609-11623, doi:10.5194/acp-13-11609-2013, 2013.

Prigent, C., Papa, F., Aires, F., Jimenez, C., Rossow, W. B., and Matthews, E.: Changes in land surface water dynamics since the 1990s and relation to population pressure, *Geophys. Res. Lett.*, 39, L08403, doi:10.1029/2012GL051276, 2012.

Riley, W. J., Subin, Z. M., Lawrence, D. M., Swenson, S. C., Torn, M. S., Meng, L., Mahowald, N. M., and Hess, P.: Barriers to predicting changes in global terrestrial methane fluxes: analyses using CLM4Me, a methane biogeochemistry model integrated in CESM, *Biogeosciences*, 8, 1925-1953, doi:10.5194/bg-8-1925-2011, 2011.

Saatchi, S. S., Harris, N. L., Brown, S., Lefsky, M., Mitchard, E. T., Salas, W., Zutta, B. R., Buermann, W., Lewis, S. L., Hagen, S., Petrova, S., White, L., Silman, M., and Morel, A.: Benchmark map of forest carbon stocks in tropical regions across three continents, *P. Natl. Acad. Sci.*, 108, 9899–9904, doi: 10.1073/pnas.1019576108, 2011.

Schimel, D., Stephens, B. B., and Fisher, J. B.: Effect of increasing CO2 on the terrestrial carbon cycle, *Proc. Natl. Acad. Sci.*, 112, 436–441, doi:10.1073/pnas.1407302112, 2015a.

Schimel, D., Pavlick, R., Fisher, J. B., Asner, G. P., Saatchi, S., Townsend, P., Miller, C., Frankenberg, C., Hibbard, K., and Cox, P.: Observing terrestrial ecosystems and the carbon cycle from space, *Glob. Change Biol.*, 21, 1762–1776, doi:10.1111/gcb.12822, 2015b.

Schroeder, R., McDonald, K. C., Chapman, B. D., Jensen, K., Podest, E., Tessler, Z. D., Bohn, T. J., and Zimmermann, R.: Development and Evaluation of a Multi-Year Fractional Surface Water Data Set Derived from Active/Passive Microwave Remote Sensing Data. *Remote Sensing*, 7, 16688-16732, doi:10.3390/rs71215843, 2015.

Skamarock, W. C. and Klemp, J. B.: A time-split nonhydrostatic atmospheric model for weather research and forecasting applications, *J. Comput. Phys.*, 227, 3465–3485, doi:10.1016/j.jcp.2007.01.037, 2008.

Sweeney, C., Karion, A., Wolter, S., Newberger, T., Guenther, D., Higgs, J. A., Andrews, A. E., Lang, P. M., Neff, D., Dlugokencky, E., Miller, J. B., Montzka, S. A., Miller, B. R., Masarie, K. A., Biraud, S. C., Novelli, P. C., Crotwell, M., Crotwell, A. M., Thoning, K., and Tans, P. P.: Seasonal climatology of CO_2 across North America from aircraft measurements in the NOAA/ESRL Global Greenhouse Gas Reference Network, *J. Geophys. Res. Atmos.*, 120, doi:10.1002/2014JD022591, 2015.

Turner, A. J., Jacob, D. J., Wecht, K. J., Maasakkers, J. D., Lundgren, E., Andrews, A. E., Biraud, S. C., Boesch, H., Bowman, K. W., Deutscher, N. M., Dubey, M. K., Griffith, D. W. T., Hase, F., Kuze, A., Notholt, J., Ohyama, H., Parker, R., Payne, V. H., Sussmann, R., Sweeney, C., Velazco, V. A., Warneke, T., Wennberg, P. O., and Wunch, D.: Estimating global and North American methane emissions with high spatial resolution using GOSAT satellite data, *Atmos. Chem. Phys.*, 15, 7049-7069, doi:10.5194/acp-15-7049-2015, 2015.

Uliasz, M.: Lagrangian particle modeling in mesoscale applica- tions, *Environmental Modelling II*, ed. P. Zanetti, Computational Mechanics Publications, 71–102, 1994.

Vukicevic, T., Braswell, B. H., and Schimel, D.: A diagnostic study of temperature controls on global terrestrial carbon exchange, *Tellus, Ser. B*, 53, 150–170, doi:10.1034/j.1600-0889.2001.d01-13.x, 2001.

Wecht, K. J., Jacob, D. J., Sulprizio, M. P., Santoni, G. W., Wofsy, S. C., Parker, R., Bösch, H., and Worden, J.: Spatially resolving methane emissions in California: constraints from the CalNex aircraft campaign and from present (GOSAT, TES) and future (TROPOMI, geostationary) satellite observations, *Atmos. Chem. Phys.*, 14, 8173-8184, doi:10.5194/acp-14-8173-2014, 2014.

Whalen, S. C.: Biogeochemistry of methane exchange between natural wetlands and the atmosphere, *Environ. Eng. Sci.*, 22, 73–94, doi:10.1089/ees.2005.22.73, 2005.

Wania, R., Ross, I., and Prentice, I. C.: Implementation and evaluation of a new methane model within a dynamic global vegetation model: LPJ-WHyMe v1.3.1, *Geosci. Model Dev.*, 3, 565-584, doi:10.5194/gmd-3-565-2010, 2010.

Wilson, C., Gloor, M., Gatti, L. V., Miller, J. B., Monks, S. A., McNorton, J., Bloom, A. A., Basso, L. S., and Chipperfield, M. P.: Contribution of regional sources to atmospheric methane over the Amazon Basin in 2010 and 2011. *Global Biogeochem. Cy.*, 30, doi:10.1002/2015GB005300, 2016.

Worden, J., Kulawik, S., Frankenberg, C., Payne, V., Bowman, K., Cady-Peirara, K., Wecht, K., Lee, J.-E., and Noone, D.: Profiles of CH4, HDO, H2O, and N2O with improved lower tropospheric vertical resolution from Aura TES radiances, *Atmos. Meas. Tech.,* 5, 397-411, doi:10.5194/amt-5-397-2012, 2012.

Yokota, T., Yoshida, Y., Eguchi, N., Ota, Y., Tanaka, T., Watanabe, H., and Maksyutov, S.: Global concentrations of CO_2 and CH_4 retrieved from GOSAT: First preliminary results, SOLA, 5, 160– 163, doi:10.2151/sola.2009-041, 2009.

Atmos. Chem. Phys. Discuss., doi:10.5194/acp-2016-325, 2016
Manuscript under review for journal Atmos. Chem. Phys.
Published: 27 April 2016

Atmospheric Chemistry and Physics Discussions

Tables

Table 1: Observation system characteristics[a]

Observation System	Single sounding footprint size	Single CH_4 measurement precision	Visits per day
LEO	7km × 7km	0.6% (10.8 ppb)	1
GEO	3km × 3km	0.6% (10.8 ppb)	4
LEO+[b]	7km × 7km	0.42% (7.6 ppb)	1
GEO×2	3km × 3km	0.6% (10.8 ppb)	8
GEO-Z1	3km × 3km	0.6% (10.8 ppb)	4[c]
GEO-Z2	3km × 3km	0.6% (10.8 ppb)	4[d]

[a]LEO and GEO observation parameters are broadly consistent with TROPOMI and GEOCAPE simulations by Wecht et al.,(2014); to simplify comparisons, we set GEO and LEO default single CH_4 sounding precision to 0.6%.

[b]Single measurement precision is a factor of $\sqrt{2}$ higher than LEO; this is the equivalent to doubling the visits per day for LEO.

[c]2 (6) visits per day in 0 – 50%ile (50 – 100%ile) cloud-cover areas;

[d]2 (10) visits per day in 0 – 75%ile (75 – 100%ile) cloud-cover areas;

Atmos. Chem. Phys. Discuss., doi:10.5194/acp-2016-325, 2016
Manuscript under review for journal Atmos. Chem. Phys.
Published: 27 April 2016

Atmospheric Chemistry and Physics Discussions

Figures

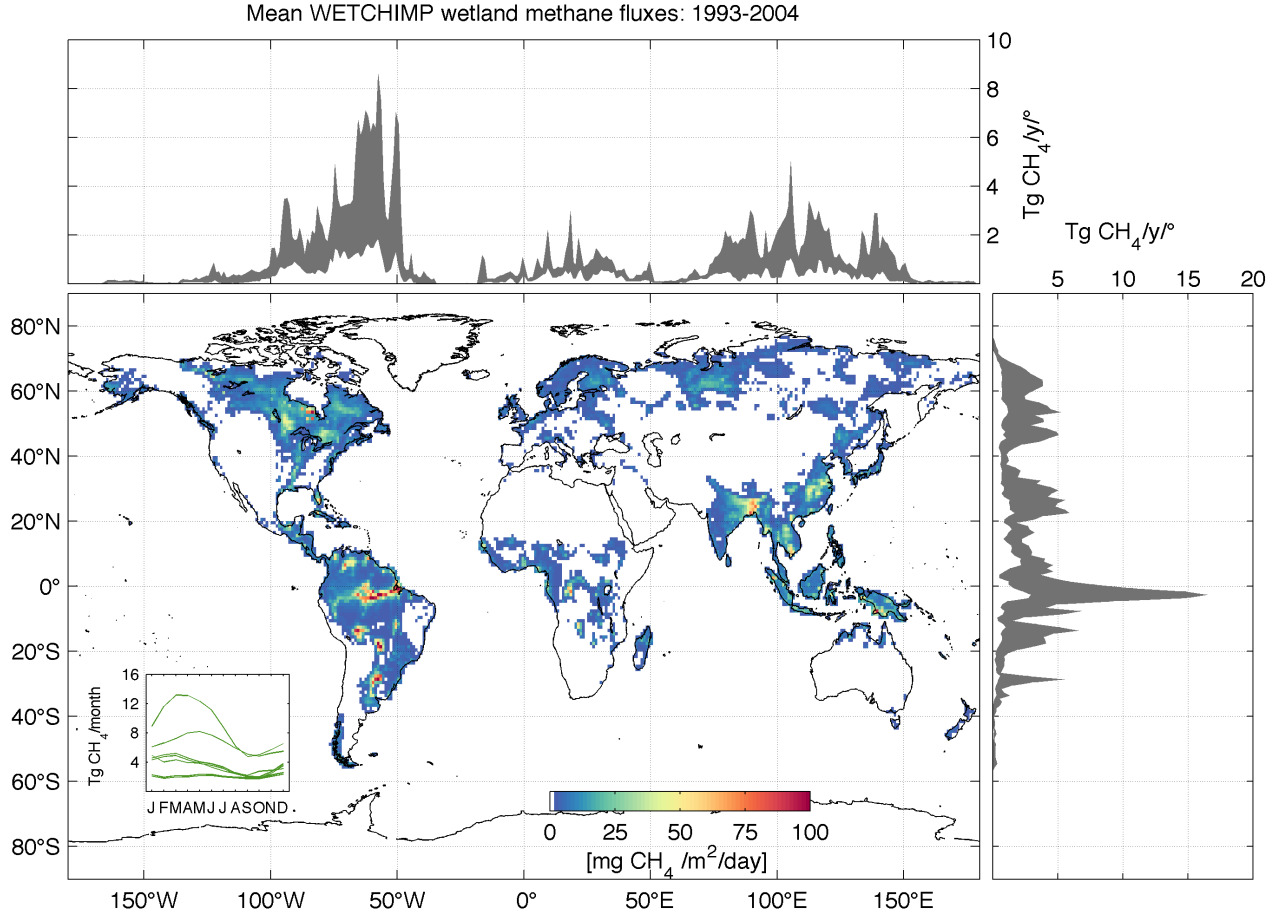

Figure 1: Mean annual wetland and rice CH_4 emissions (central maps), and associated longitudinal and latitudinal uncertainty (grey bands), based on the WETCHIMP model inter-comparison project (Melton et al., 2013). **Inset**: Average WETCHIMP model Amazon basin monthly CH_4 emissions.

Atmos. Chem. Phys. Discuss., doi:10.5194/acp-2016-325, 2016
Manuscript under review for journal Atmos. Chem. Phys.
Published: 27 April 2016

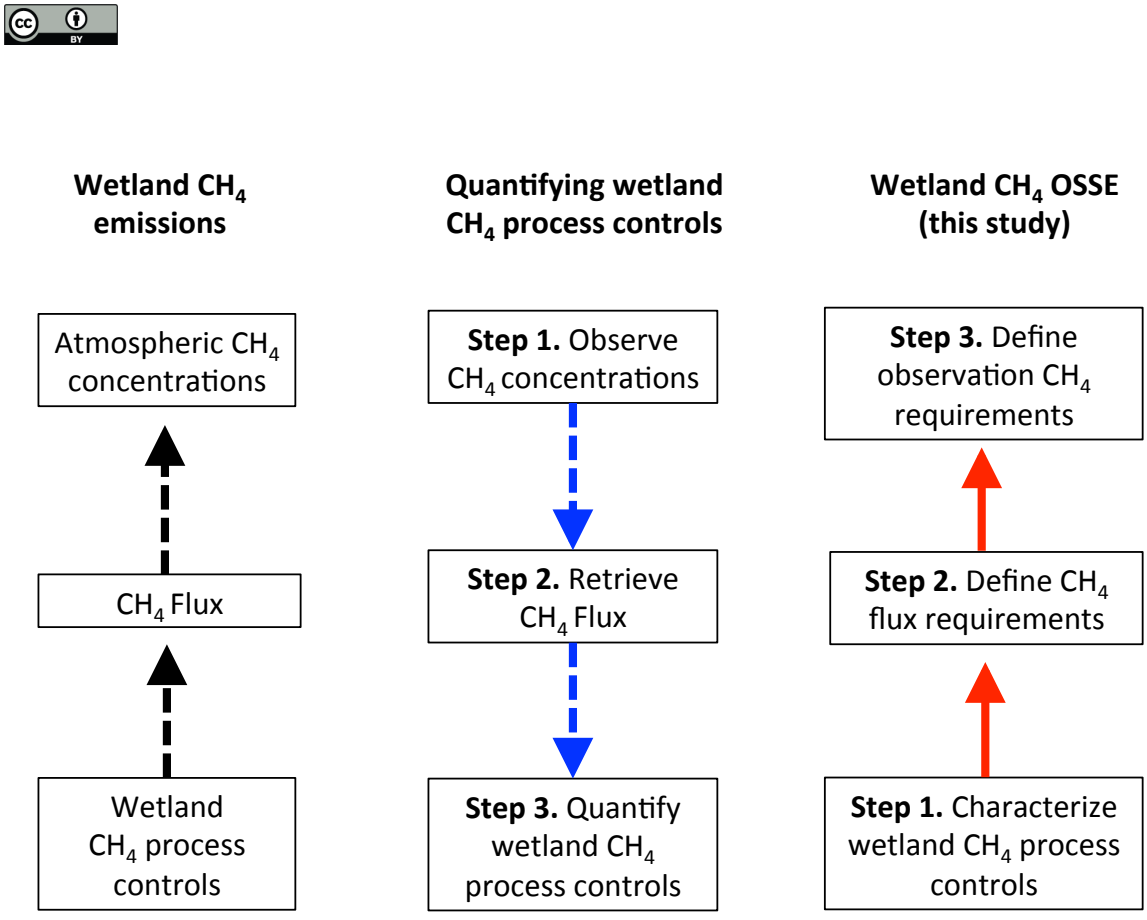

Figure 2. Wetland CH_4 emissions into the atmosphere are regulated by wetland biogeochemical processes (left column). Continental-scale wetland CH_4 process controls can be retrieved by (i) resolving surface CH_4 fluxes from retrieved satellite CH_4 observations; (ii) resolving process parameters from retrieved CH_4 fluxes (middle column). The optimal satellite CH_4 observation requirements are a function of the flux resolution and precision required to resolve wetland CH_4 process controls (right column): OSSE steps 1-3 are described in sections 2.1-2.3.

Atmos. Chem. Phys. Discuss., doi:10.5194/acp-2016-325, 2016
Manuscript under review for journal Atmos. Chem. Phys.
Published: 27 April 2016

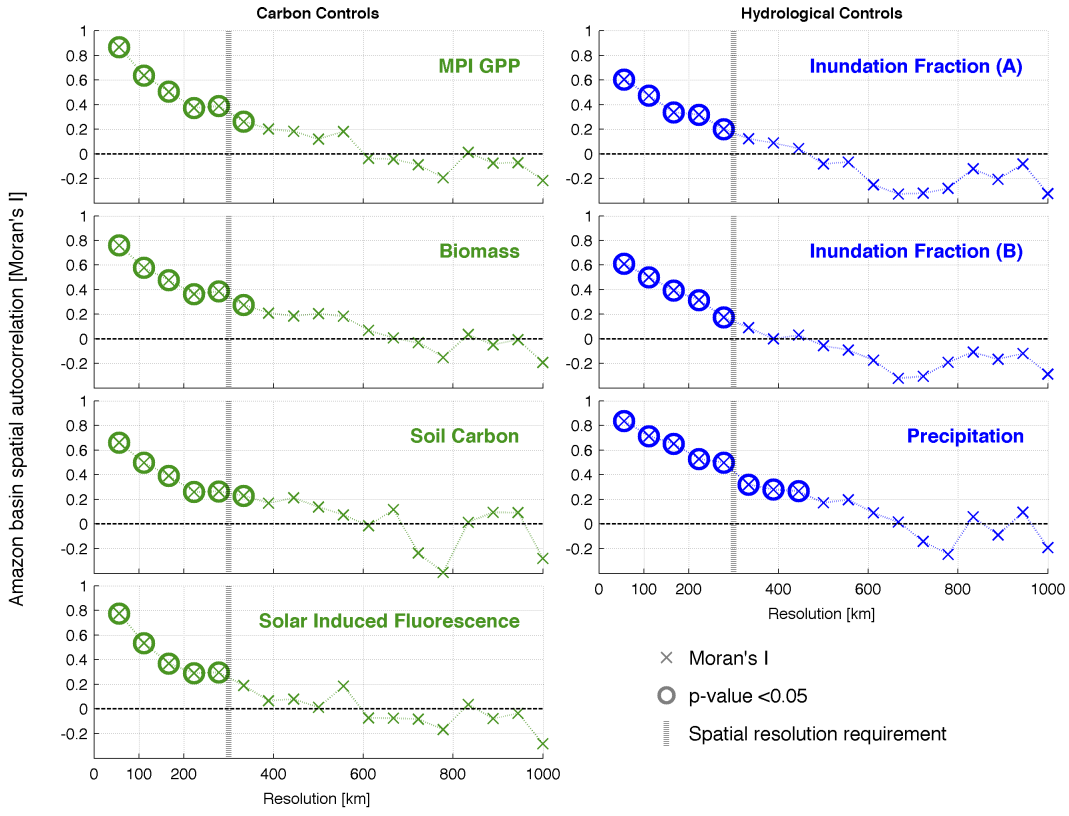

Figure 3: Spatial autocorrelation (Moran's I) for potential carbon controls (left column) and hydrological controls (right column) on wetland CH_4 emissions. The spatial variability of carbon controls are derived from satellite observations (Biomass, Saatchi et al., 2011; solar induced fluorescence; Joiner et al., 2013), the Harmonized World Soil database (soil carbon, Hiederer & Köchy, 2011) and FLUXNET derived GPP (Jung et al., 2009). The spatial variability estimates for hydrological controls are based on satellite measurements of inundation (A: Prigent et al., 2007; B: Schroeder et al., 2015), and precipitation (the NASA Tropical Rainfall Measuring Mission). Significant Moran's I values (where the Moran's I p-value < 0.05) are highlighted as circles. We set a 300km spatial resolution requirement for monthly CH_4 flux retrievals, based on the maximum correlation lengths of potential carbon and hydrological controls on wetland CH_4 emissions. The spatial datasets and the details of the Moran's I analysis are fully described in Appendix A.

Atmos. Chem. Phys. Discuss., doi:10.5194/acp-2016-325, 2016
Manuscript under review for journal Atmos. Chem. Phys.
Published: 27 April 2016

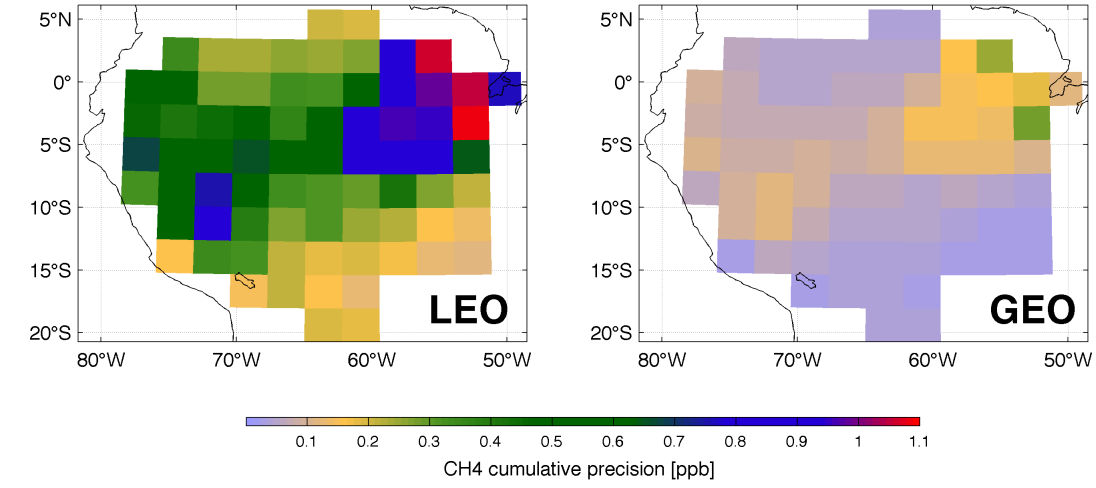

Figure 4: Retrieved monthly CH_4 cumulative measurement precision at a 300km × 300km resolution for LEO and GEO observing systems (OS); the OS configurations are described in Table 1.

Atmos. Chem. Phys. Discuss., doi:10.5194/acp-2016-325, 2016
Manuscript under review for journal Atmos. Chem. Phys.
Published: 27 April 2016

Atmospheric Chemistry and Physics Discussions

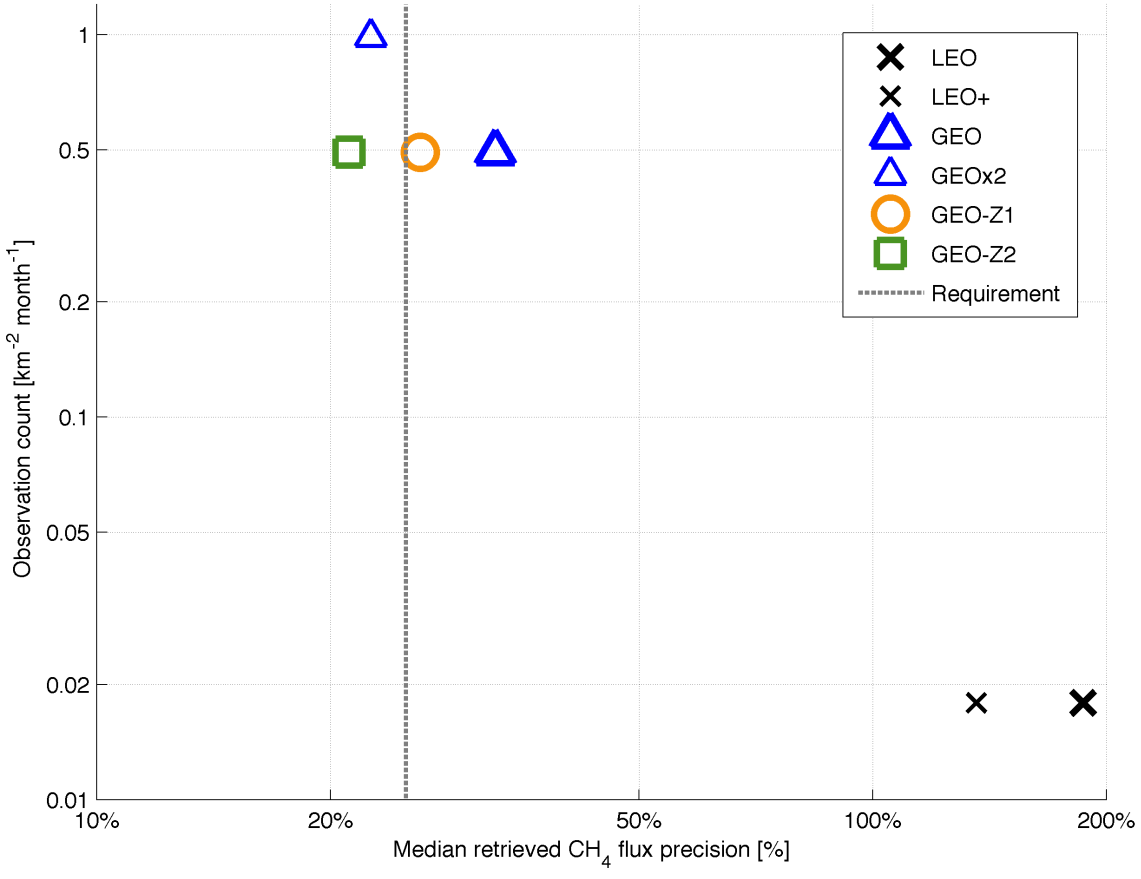

Figure 5: CH_4 observations density (observations per unit area; y-axis) versus retrievable 300km × 300km flux precision (x-axis) for six CH_4 observation systems (see Table 1 for details).

Atmos. Chem. Phys. Discuss., doi:10.5194/acp-2016-325, 2016
Manuscript under review for journal Atmos. Chem. Phys.
Published: 27 April 2016

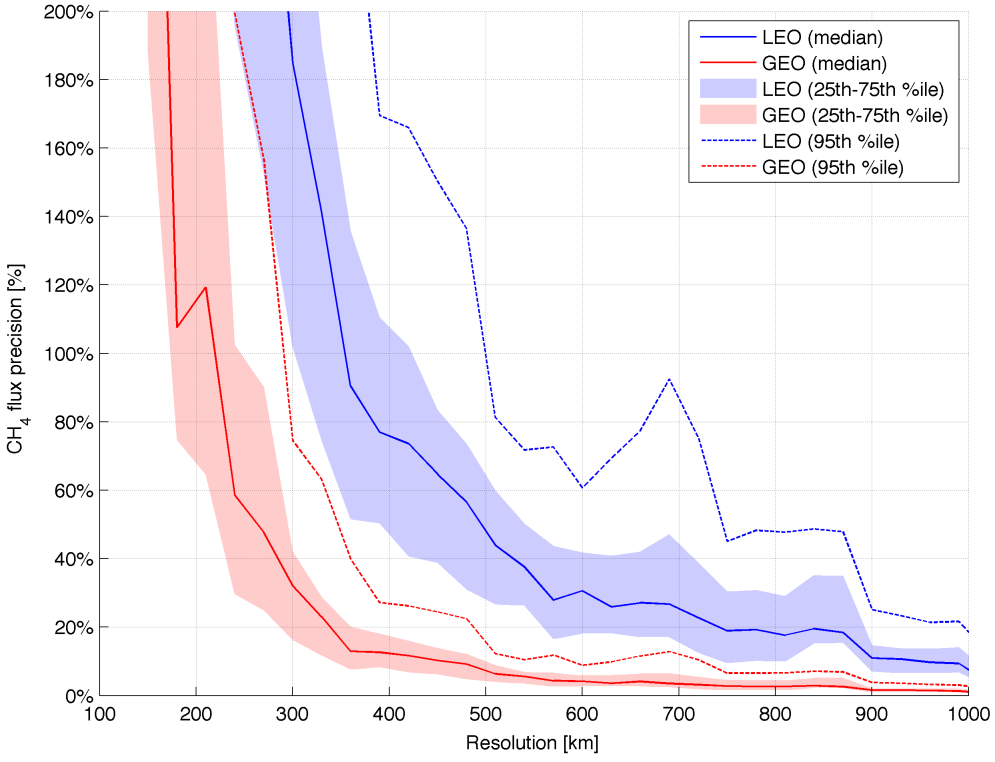

Figure 6: Retrieved flux precision cumulative CH_4 measurement precision for LEO and GEO for L = 150 – 990km. See table 1 for details on GEO and LEO CH_4 observing systems.

Atmos. Chem. Phys. Discuss., doi:10.5194/acp-2016-325, 2016
Manuscript under review for journal Atmos. Chem. Phys.
Published: 27 April 2016

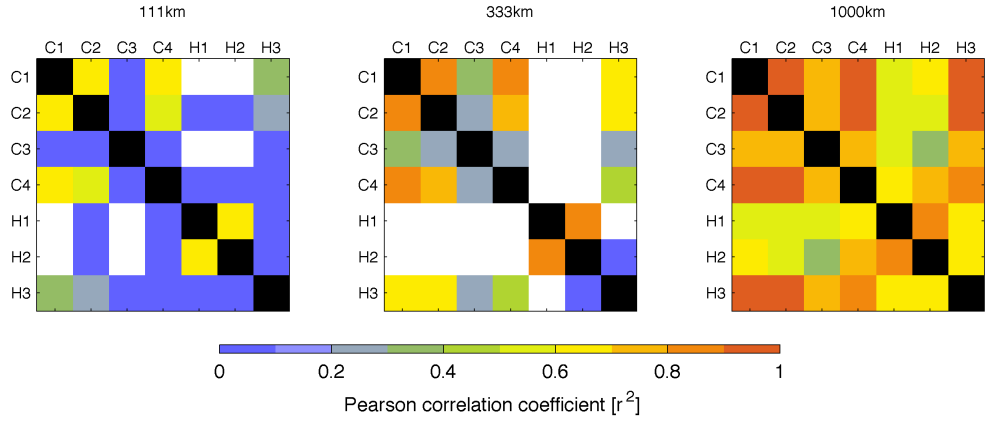

Figure A1: Pearson's correlation coefficient (r^2) values between wetland CH_4 emission carbon (C) and hydrological (H) process controls (C1: MPI GPP; C2 biomass; C3 soil carbon density; C4 solar-induced fluorescence; H1 Inundation fraction A; H2 inundation fraction B; H3 precipitation). White squares denote insignificant correlations ($p_{value} > 0.05$) and black squares denote the correlation matrix diagonal ($r^2 = 1$).

Atmos. Chem. Phys. Discuss., doi:10.5194/acp-2016-325, 2016
Manuscript under review for journal Atmos. Chem. Phys.
Published: 27 April 2016

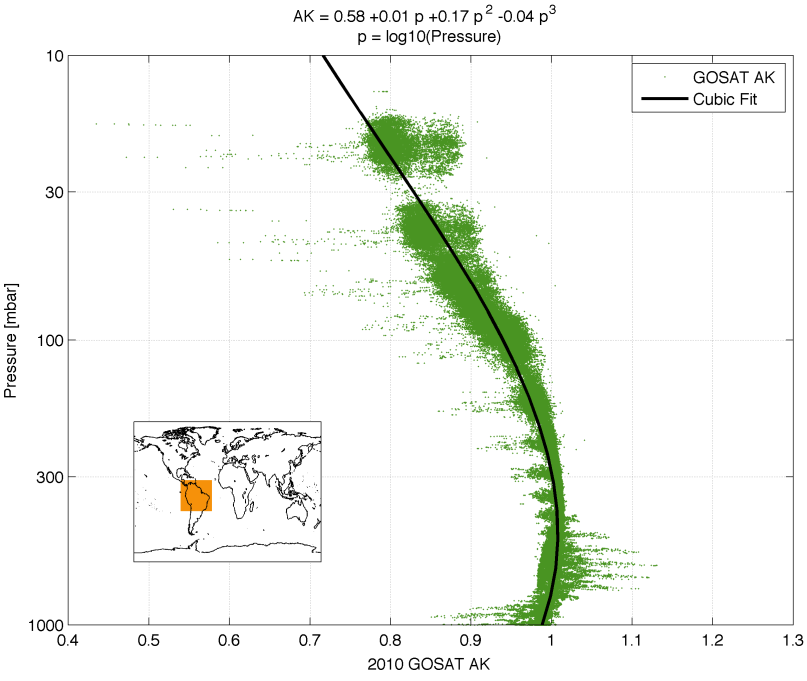

Figure A2. January to December 2010 GOSAT averaging kernels (AK) for the broader Amazon region (green dots). The black line denotes the AK cubic fit (w.r.t. pressure *p*; equation shown at the top of the figure). This AK was used to vertically weight the LPDM footprint and sample WRF CH_4 concentrations (see Appendix C).

Atmos. Chem. Phys. Discuss., doi:10.5194/acp-2016-325, 2016
Manuscript under review for journal Atmos. Chem. Phys.
Published: 27 April 2016

Atmospheric Chemistry and Physics Discussions

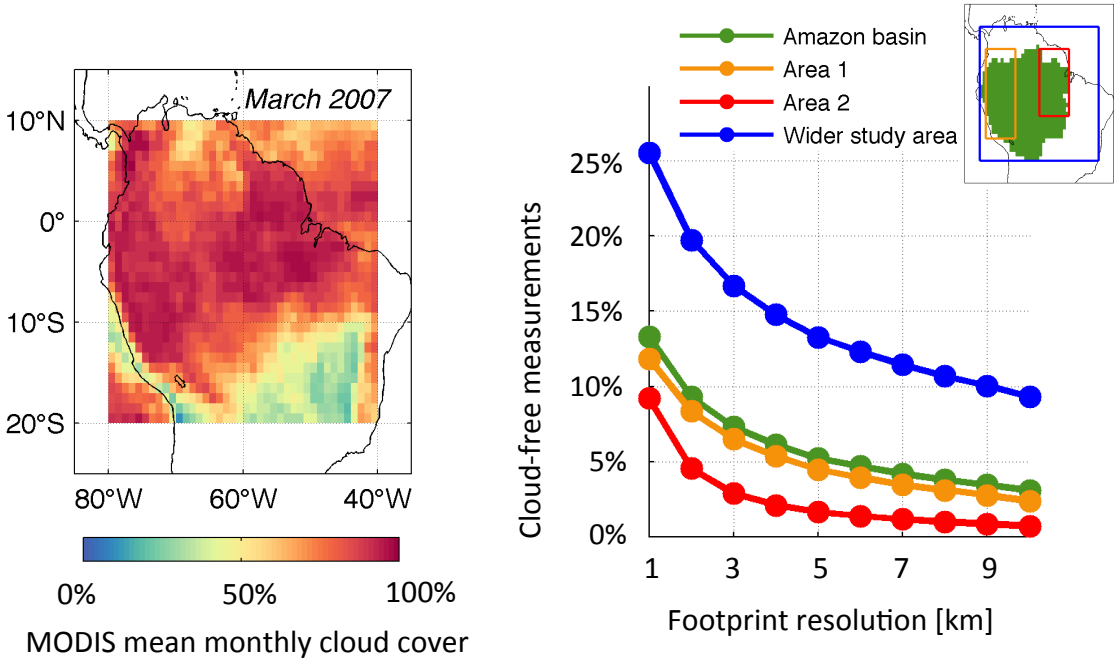

Figure B1. **Left:** March 2007 mean MODIS cloud cover aggregated to 1° ×1°. **Right:** Summary of cloud-free observations versus footprint size for the broader study area, the Amazon river basin, and two sub-regions (east and west Amazon river basin).

5

Atmos. Chem. Phys. Discuss., doi:10.5194/acp-2016-325, 2016
Manuscript under review for journal Atmos. Chem. Phys.
Published: 27 April 2016

Atmospheric Chemistry and Physics Discussions

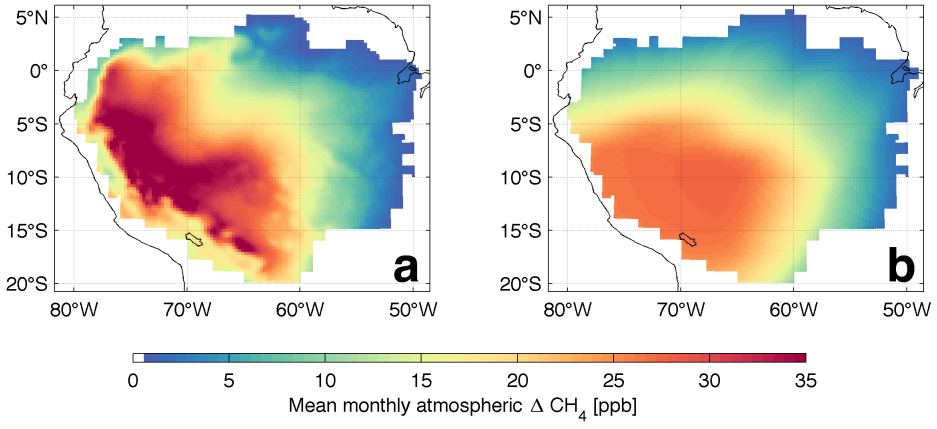

Figure C1. March 2007 simulations of atmospheric CH_4 concentration enhancements – based on 12 mg m^{-2} day^{-1} fluxes throughout the Amazon basin – derived using the WRF atmospheric transport model (**a**) and the LPDM influence function approach (**b**).

5